

Advanced Eyesafe Lidar for Atmospheric Wind Measurements

Sammy Henderson^a, Michael Kavaya^b, Jirong Yu^b, Pat Kratovil^a, Charley Hale^a, Joe Diamond^a, Dale Bruns^a, Larry Petway^b, John Marketon^b, Dave Emmitt^c, Zhaoyan Liu^b and Kris Bedka^b

^a Beyond Photonics, 6205 Lookout Rd., Ste B, Boulder, CO

^b NASA LaRC, 5 N. Dryden Street, Mail 468, Hampton, VA

^c Simpson Weather Associates, 809 East Jefferson Street, Charlottesville, VA
sammy@beyondphotonics.com

Abstract: A high-performance 2-micron wavelength coherent lidar system has been developed for measurement of atmospheric winds. The lidar transceiver incorporates several technologies which make an engineered-for-space version of it a candidate for future space-based operation. These technologies include: a high-power in-band-pumped transmitter; compact highly-stable reference lasers that enable precision wind measurement at long range and removal of large orbital-induced Doppler shifts; autonomous alignment capability ensuring that both the transmitter and lidar receiver maintain alignment after shock or environmentally-induced misalignments; lag angle correction to correct for platform rotation between transmit and receive time; and electro-optic beam path switching allowing for simultaneous fast switching of the transmit and receive beam paths between two independent lidar views. The lidar has been used for ground-based wind measurements and it is planned for airborne operation.

Keywords: Coherent Laser Radar, Lidar, Wind Measurement

1. Introduction

Coherent detection wind lidar systems have proven very effective for high-accuracy high-spatial-resolution wind measurements for many applications from both ground and airborne platforms [1-3]. Recently we have developed a high-performance coherent detection wind measurement lidar under the Wind-Space Pathfinder (Wind-SP) program funded by NASA's Earth Science Technology Office (ESTO). In this program, we established performance requirements and advanced several technologies needed for space-based implementation of coherent detection wind lidar systems. The technologies include: improved transmitters with high pulse energy and pulse repetition rate for long range wind measurements; auto-alignment sensors and actuators for long-term maintenance of peak coherent detection lidar performance and for removal of pointing lag angle due to platform rotation; electronic control of the transmit and receive beam path allowing for fast switching between two viewing angles (allowing vector wind measurements) with no moving parts; compact highly-stable and tunable reference lasers allowing for high-precision measurement of velocity at long ranges (>400 km) while mitigating the impact of the high velocity satellite platform; and prototype low-mass carbon-fiber-composite structures to support the lidar system.

In late 2021 these technologies were combined into a complete Wind-SP ground-based lidar demonstration system and initial ground-based wind measurements have been performed demonstrating excellent agreement with co-located ground-based wind measurements using the NASA DAWN wind lidar. During 2022, under the NASA ESTO and NASA-LaRC funded Airborne Wind Profiler (AWP) program, the ground-based demonstrator system is being improved and converted into an airborne sensor with first flights planned to begin later this year.

With additional TRL advancement a space-based lidar utilizing the Wind-SP developed and AWP-deployed technologies could allow for measurements of tropospheric winds from space.

2. Lidar Description and Measurement Capability

The key specifications of the Wind-SP ground-based lidar demonstration system are summarized in Table 1. The transmitter has a high Transmitter Figure of Merit (TFOM) which is important for

increasing the coherent detection signal to noise ratio, allowing it to operate at lower aerosol backscatter levels or to longer ranges. For a coherent detection lidar, the signal to noise ratio, after averaging over some fixed measurement time, improves linearly with the pulse energy but only as the square root of the transmitter pulse repetition frequency (PRF). For typical weak signal coherent lidar measurement scenarios the TFOM also depends weakly on the pulse duration ($\sim \tau^{0.285}$). The Wind-SP TFOM is about 40-100x larger than that of current commercially available fiber-transmitter-based lidar systems and is about 12x larger than that of the Lockheed 1.6 μm wavelength WindTracer transmitter. For a transmitter operating at 10 kHz PRF to have the same TFOM as the Wind-SP transceiver its average power would have to be about 7.1 times higher – i.e., ~81 W instead of ~11.4 W (assuming beam quality and pulse duration are held constant).

Table 1. Key Parameters of the Wind-SP Coherent Lidar

Parameter	Value	Comments
Pulse Energy (mJ)	57	variable, 25 mJ – 75 mJ (see J. Yu Paper)
PRF (Hz)	200	efficient laser with CW pump laser
Pulse FWHM Duration (ns)	180	at ~57 mJ, varies with pulse energy
Pulse Spectral Purity	Single frequency	<1.1 x Transform Limited
Transmit Beam Quality (M^2)	<1.1	high coherent detection antenna efficiency
Transmitter FOM	$> 3.1 J \cdot \sqrt{\text{Hz}} \cdot \text{ns}^{0.285}$	$TFOM = 2 / \left(1 + M^2\right) \cdot E \cdot \sqrt{PRF} \cdot \tau^{0.285}$
Transmitter Average Power (W)	11.4	up to 15 W demonstrated in lab
Wavelength (nm)	2052.92	High atm trans., easier near-DL optics
LO Frequency Jitter	< 20 kHz rms over 4 ms	$\delta V_r < 2 \text{ cm/s}$ from space due to LO
MO1/MO2 Offset Freq. wrt LO	$\pm 0.1 - 5 \text{ GHz}$, tunable	correction of space platform motion
Signal Detector / Preamp	Quantum Eff. > 0.8	Extended λ InGaAs, Dual Bal., 0.5 GHz BW
Transmitter Auto-Alignment	> 95% osc peak power	Auto-alignment of transmitter oscillator
Transmit/Receive Auto-Alignment	> 95% alignment eff.	AA of Xmit & Signal, incl. lag angle correction
T/R Beam Path	Dual-path EO Switching	Allows for fast switching between two paths
Telescope Aperture	15 cm	x 2 if beam path switching is activated
Data Acquisition	500 MS/s, 8 bits	Sufficient for 250 MHz analog BW

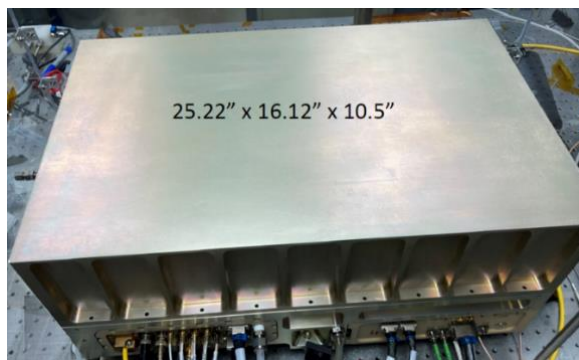


Figure 1. Wind-SP High-Power (left) & Low-Power (right) Transceiver Modules which contain the laser & optical components of the lidar except for the T/R telescope.

The Wind-SP transceiver consists of two primary laser/optical modules: the High-Power Transceiver Module and the Low-Power Transceiver Module. The embedded transmitter is described in detail in a

separate paper (see the J. Yu, et.al. paper in this conference). Photographs of the HPTM and LPTM are shown in Figure 1 and a functional diagram of the HPTM is shown in Figure 2. The LPTM is connected to the HPTM using single-mode polarization-preserving fibers and contains the low power CW lasers, the reference signal detector (whose primary purpose is to measure the frequency of the outgoing pulses), and the fiber coupling, routing, and switching components. The CW lasers within the LPTM are a frequency-stable local oscillator, two frequency-offset master oscillators, and a 1.5-micron wavelength laser diode that is used as part of the transmit/receive auto-alignment subsystem.

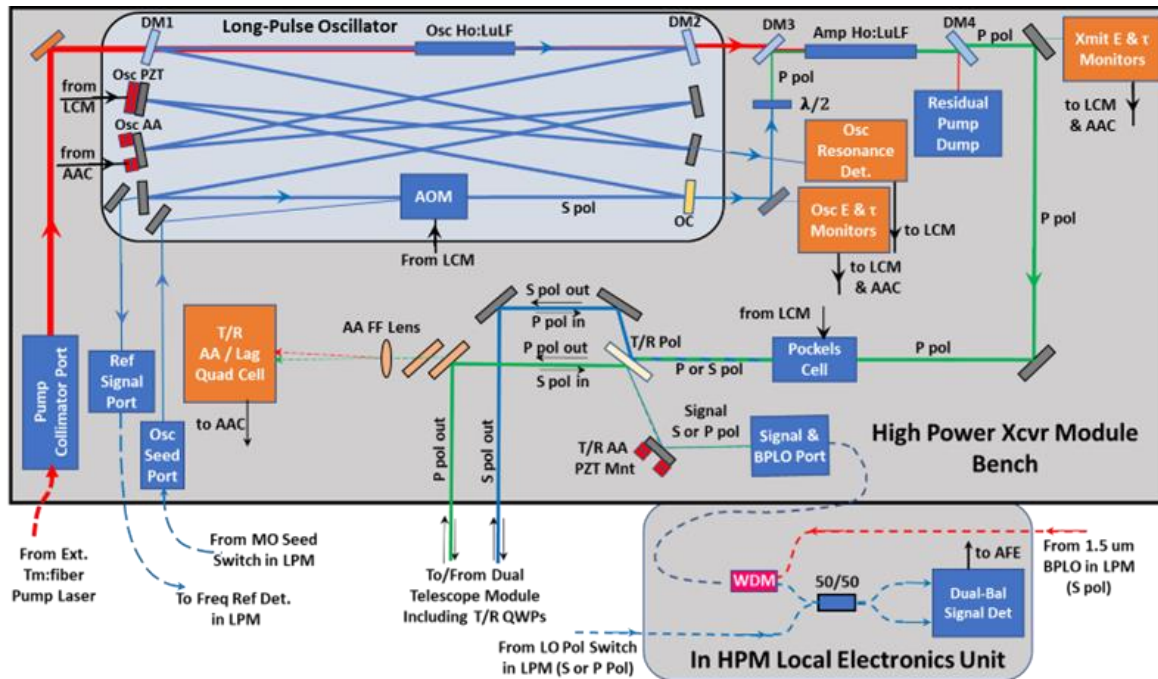


Figure 2. Functional diagram of the High-Power Transceiver Module.

The Wind-SP lidar system has already been utilized to measure winds from the ground. One example of line-of-sight wind speed and signal-to-noise ratio (aerosol backscatter dependent) profiles measured over Hampton, VA during a 2.5-hour period on April 30, 2022, is provided in Figure 3. For this measurement the transmitter power was reduced to about 30 mJ – out of an abundance of caution due to a low damage threshold mirror in the lidar system. The signals for a 10 s period (2000 pulses) were averaged for each measurement update in this example. The lidar line of sight (LOS) throughout these measurements was fixed at an elevation angle of about 62 degrees and an azimuth angle of about 27 degrees east of due north. Horizontal wind speeds were light (< 5 m/s) and complex layering of wind flows are evident. The PBL is approximately 1 km deep, as evidenced by the narrow layer of higher winds at PBL top (yellow-red shading, bottom-left). A layer of enhanced aerosol concentration of unknown origin is evident above the PBL at about 2 km altitude (maroon shading, bottom-right). Three layers of clouds were observed, two distinct cirrus layers at ~9 and ~11 km in the first 45 mins of the measurement, and a very optically thick stratiform layer at 3.5-4 km persisting for the remainder of the period. Prior to the arrival of the stratiform layer, the Wind-SP system retrieved an almost continuous wind profile up to the cirrus clouds from the background aerosol conditions even at the reduced pulse energy. The vertical line at UTC time of about 18.2 hours indicates the time when we switched the lidar from its P polarized beam path to its S polarized beam path both viewing along the same LOS. Both beam paths have the desired nearly identical measurement sensitivity.

To emulate the space-based vector wind measurement geometry using two look directions, we have also directed the two beam paths from Wind-SP along two independent LOS separated by 90 degrees in azimuth with both having an elevation angle of about 60 degrees. The data along these two LOS is processed to extract wind speed and direction vs altitude. The two-look Wind-SP measurement (*not shown here*) shows excellent agreement with independent wind measurements using the NASA DAWN lidar system which uses a scanner to scan over 5 azimuth positions for estimation of the wind profiles.

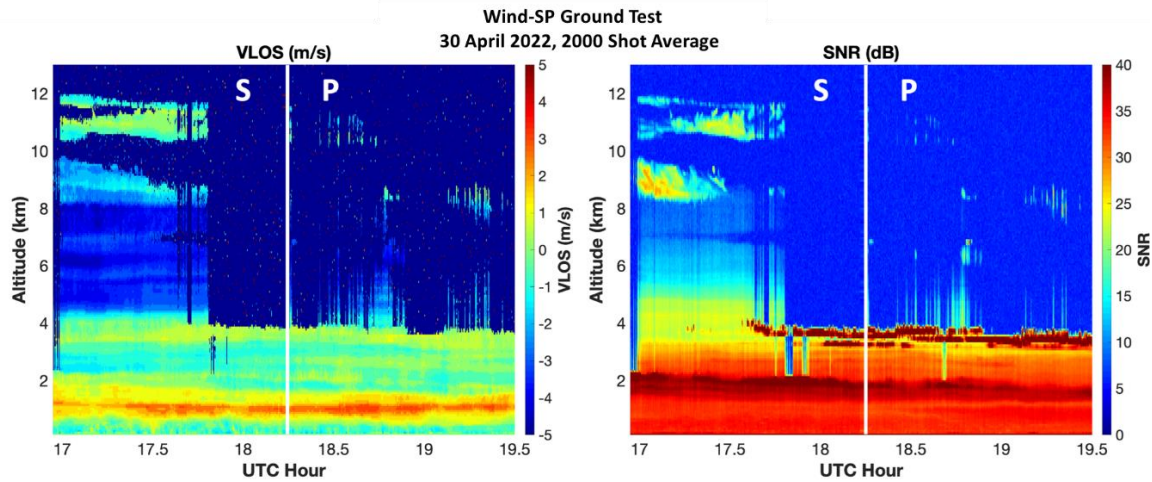


Figure 3. Example line of sight wind measurements from the ground using the Wind-SP lidar.

We are currently continuing to improve the ground-based Wind-SP demonstrator system and will soon be integrating it with other components needed for airborne operation. A diagram of the primary assembly of the planned Airborne Wind Profile (AWP) instrument is provided in Figure 4 (left). Laser pulses from the two Wind-SP beam paths are directed downward through parallel 15 cm diameter beam expanders. One beam is sent through a rotating scanner prism where it is directed 30° off-nadir, providing for vertical profiles of horizontal winds at selectable height resolution. While the scanner is rotating from one azimuth angle to another, the second beam path becomes active which is directed in the nadir direction, providing a direct measurement of vertical wind speeds vs altitude.

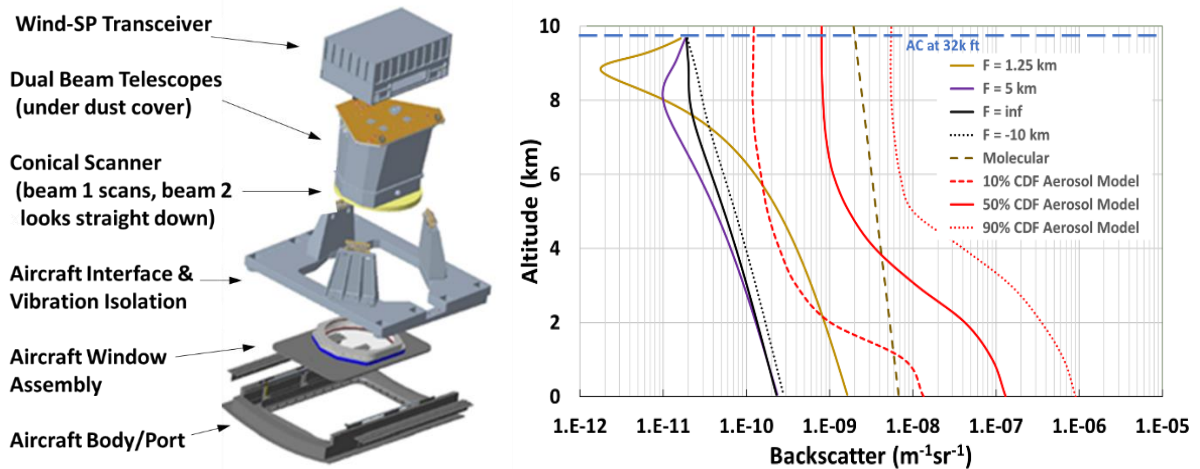


Figure 4. Left: A diagram of key elements of the Airborne Wind Profiler (AWP) Instrument. Right: Estimated minimum backscatter sensitivity vs altitude, parametric in various telescope focus settings, for 32k ft aircraft altitude, compared to aerosol backscatter models.

The calculated minimum backscatter sensitivity of AWP vs altitude as compared to aerosol backscatter models is illustrated in Figure 4 (right). The instrument is expected to provide continuous coverage from the aircraft to the ground in the absence of thick cloud cover most of the time, with aerosol backscatter rarely dropping below the sensitivity level of the lidar. The yellow-brown curve in the figure represents the case where the beam is focused close to the aircraft ($F = 1.25$ km), allowing for very low minimum backscatter sensitivity of $\approx 2 \times 10^{-12} m^{-1}sr^{-1}$ just below the aircraft.

With a larger telescope, a space-hardened version of the Wind-SP lidar could make wind measurements from a space-based platform. We have modeled the minimum aerosol backscatter sensitivity from space, as is illustrated in Figure 5, assuming the Wind-SP lidar technology, a 400 km satellite platform, and a 1 m diameter aperture. There is a large variation in the level of aerosol backscatter as is illustrated in the left panel of Figure 5. If the aerosol backscatter is above a given minimum sensitivity curve, then

successful wind measurements can be obtained at that resolution. In the boundary layer, the aerosol backscatter is strong allowing for high resolution measurements. In very clear air (Background) conditions in the mid and upper troposphere, the aerosol backscatter can be very low requiring signal integration over larger horizontal and vertical extent to successfully make accurate wind measurements. When the aerosol loading in the mid and upper troposphere is larger (Enhanced), higher resolution measurements are possible at the higher altitudes. The lidar is always able to make useful measurements from clouds, and in the case of subvisual cirrus, through the depth of the cloud. The minimum backscatter sensitivity assuming high, moderate, and low spatial resolution measurements vs altitude is illustrated in Figure 5 (right). Examples of each of these resolution levels are: High, 0.25 km vertical over 30 km horizontal, easily achieved in boundary layer, clouds, and other elevated aerosol layers; Mid, 1 km vertical over 80 km horizontal, possible in mid and upper troposphere in elevated backscatter conditions; and Low, 4 km vertical over 400 km horizontal, appropriate for upper troposphere and lower stratosphere. The dashed lines show the significant improvement in sensitivity that is afforded if the lidar utilized the same orbit altitude and aperture as the Aeolus wind lidar (320 km and 1.5m).

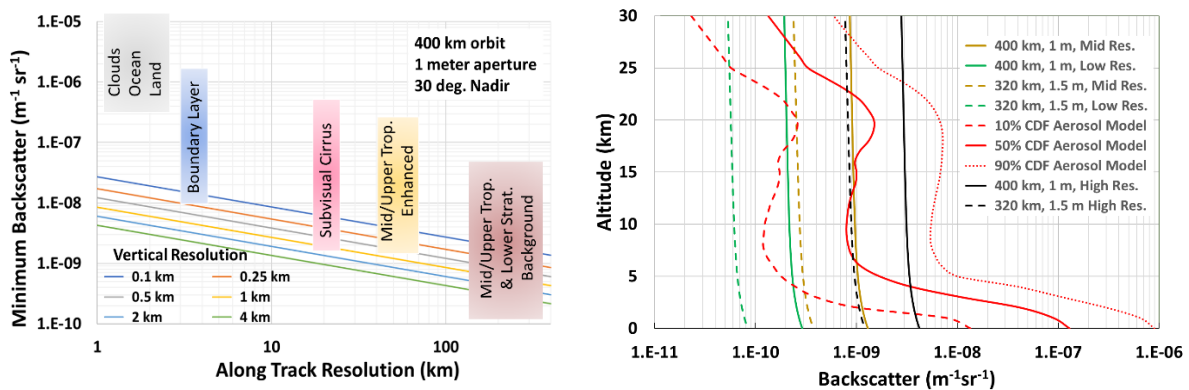


Figure 5. Left: minimum backscatter sensitivity of Wind-SP at 10 km altitude assuming a 30-degree nadir angle with the lidar at 400 km and using a 1 m diameter aperture. Right: Minimum backscatter vs altitude compared to aerosol backscatter models. Solid lines for 400 km altitude and 1 m optics and dashed lines for Aeolus-like orbit and altitude (320 km and 1.5 m).

3. Summary and Acknowledgments

A high-performance 2-micron wavelength coherent lidar system has been developed for measurement of atmospheric winds. The lidar has demonstrated initial wind measurements from the ground and is planned for airborne wind measurements. With continued improvements and TRL advancement the lidar could provide useful measurements from space.

This work was supported under the ESTO Wind-SP program, Parminder Ghuman manager. Others who contributed to the program that are not in the author list were David Macdonnell, Alan Little, Keith Murray, Chris Edwards, Dave D'Epagnier, Neil Vanasse, Teh-Hwa Wong, Joy Cotie, Geoff Wilson, Kevin Williamson, Steve Greco, Aboubakar Traore, Songsheng Chen, and Anna Noe.

4. References

- [1] S.W. Henderson, P. Gatt, D. Rees, and R.M. Huffaker, **Wind Lidar**, book chapter in *Laser Remote Sensing*, Eds. Fujii and Fukuchi, CRC Press, Taylor & Francis Group, Boca Raton, FL, p 469-722, (2005)
- [2] Kavaya, M., et al, "The Doppler Aerosol Wind (DAWN) Airborne, Wind-Profiling Coherent-Detection Lidar System: Overview and Preliminary Flight Results", *J. Atmos. Ocean. Tech.*, 31, 826–842, 2014.
- [3] M. Weissmann, R. Busen, A. Dombrack, S. Rahm, and O. Reitebuch, "Targeted observations with an airborne wind lidar," *J. Atmos. Oceanic Tech.* 22, 1706-1719 (2005)